Progress In Electromagnetics Research, PIER 84, 205–220, 2008

EMC ANALYSIS OF ANTENNAS MOUNTED ON ELECTRICALLY LARGE PLATFORMS WITH PARALLEL FDTD METHOD

J.-Z. Lei, C.-H. Liang, W. Ding, and Y. Zhang

National Key Laboratory of Antennas and Microwave Technology
Xidian University
Xi'an, Shaanxi 710071, China

Abstract—In this paper, the Parallel Finite-Difference Time-Domain (FDTD) method based on MPI (Message Passing Interface) is applied to analyze the EMC problems of the electrically large platforms accurately and quickly, which is a full-wave numerical method. The MPI library and domain decomposition method are applied to implement the Parallel FDTD method, so that the computation resource is expanded. The method can analyze the EMC problems by modeling the electrically large platforms accurately. Then the network theory is introduced to compute the isolation between antennas combined with the Parallel FDTD method firstly, which avoids the complexity of sweeping frequency and reduce the computing time greatly. Numerical results show that the method is correct and efficient. Finally, the EMC problems of antennas mounted on electrically large platforms are analyzed and some useful conclusions are obtained.

1. INTRODUCTION

The EMC problems of electrically large targets is computationally very demanding. The mutual coupling effects between antennas and platforms play a very important role in the areas of EMC. They will change the input impedance of each antenna, cause power to be reflected to the feed structures, and affect the antenna radiation patterns and polarization, which may degrade the antenna performance and cause electromagnetic interference problems in communication systems. Therefore, computing radiation patterns and isolation between antennas is a crucial issue and should be taken into account before mounting antennas.

In the past, various methods have been used for the EMC problems of electrically large targets. MOM (method of moment) [1], a general and reliable low-frequency method, has inferior efficiency when electrically large complex targets are analyzed. The high-frequency methods, such as PO (physical optics) [2], GTD (The geometrical theory of diffraction) and UTD (The uniform geometrical theory of diffraction) [3], is accurate relatively for the wave band above 1 GHz. However they are not applicable for the short and ultrashort wave band obviously, and they can't be used to analyze the near field character of antennas. Also, parallel MLFMA [4] is efficient to analyze the electromagnetic problems of electrically large targets. In addition, all the algorithms above are frequency-domain analysis so that too multiple calculation is needed when sweeping frequency is essential.

FDTD is a powerful numerical technique, which is currently used for the analysis of a wide variety of EM field problems such as radiation and scattering of electromagnetic field, microwave and millimeter wave circuits and EMC etc where it has achieved greatly successful applications [5–9]. As a full wave numerical method [10], FDTD can solve the electromagnetic problems accurately through simulating all the physical process of electromagnetic wave [11, 12]. Besides, FDTD can avoid the complexity of sweeping frequency through Fourier Transforming the time-domain data [13, 14]. On the other hand, FDTD requires large amounts of computer memory and long simulation time, which become the limiting factors when it is used to solve electromagnetic field problems of objects with electrically large size.

Parallel FDTD method is an effective way to solve the issues [15, 16]. This paper adopts MPI-based Parallel FDTD to analyze the EMC problems of Electrically Large Complex Platforms efficiently [17]. Besides, the network theory is introduced to compute the isolation between antennas combined with the Parallel FDTD method firstly. Using Parallel FDTD method to analyze the isolation can simplify the computation and reduce the total time greatly. The EMC problems of large electrically platforms can be analyzed accurately by the method.

In Section 2, we mainly introduce the network theory to the Parallel FDTD and present how to compute the isolation between antennas. In Section 3, some examples are examined by the Parallel FDTD method. The results obtained validate it right and efficient. In Section 4, the EMC problems of several electrically large platforms are analyzed and some useful conclusions are obtained which can assist the design of electronic systems.

2. BASIC THEORY

2.1. Parallel FDTD Algorithm

In general, Parallel FDTD computation is what subdivides the whole FDTD computation space into several sub-domains [18]. Each process calculates field values in one or more sub-domains. The iterative solution of FDTD is able to continue by transferring field values across the interfaces between the neighboring processes. In short, there are three patterns to subdivide the whole space into sub-domains in Parallel FDTD, which results in three data communication patterns: 1D, 2D and 3D communication pattern of Parallel FDTD. This paper adopts 3D communication pattern, which is introduced in the following.

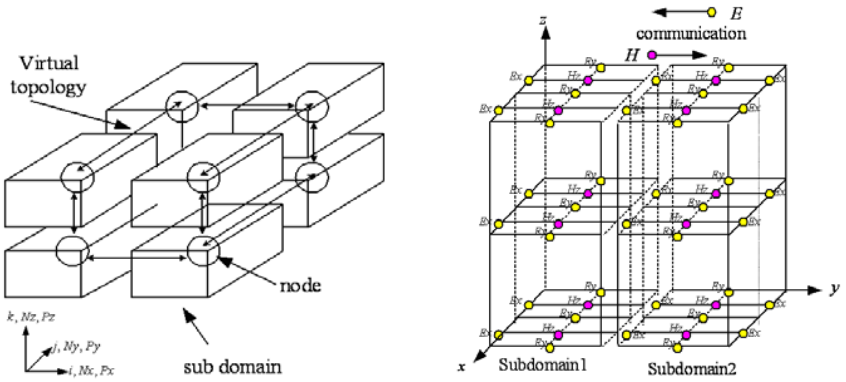

(a) partition of the simulated problem (b) field components communication

Figure 1. Division and communication of parallel FDTD in 3D.

As shown in Fig. 1(a), the computation space is subdivided into nearly equal parts in the three directions. The virtual topology of the processes' distribution is chosen in a similar shape to the problem partition. Each sub-domain is mapped to its associated node where all the field values belonging to this sub-domain are computed. To update field values lying on interfaces between sub-domains, it is necessary to transfer data between neighboring processes. A X-Z slice of the computation space at one of the interfaces between nodes in the y-direction is shown in Fig. 1(b).

The parallel code of this work is written in Fortran 90 format and run on a PC cluster that belongs to National Key Laboratory of Microwave and Antennas Technology in China. The parameters of the

Cluster are listed below:

8-Node.
Pentium IV 2.8C GHz CPU per Node
1.0 GBytes Memory per Node
1000 M High-speed Network Interface Card
1000 M Bites Switch
The photo of the PC cluster is shown in Fig. 2

Figure 2. Photo of the PC cluster.

2.2. The Network Theory

According to electromagnetic theory, a multiple-antenna system can be considered as a multiple-port network with each antenna being a port. Therefore, mutual coupling between antennas can be obtained by finding scattering parameters of the microwave network. As an example, the equivalent network for a two-antenna system is given in Fig. 3.

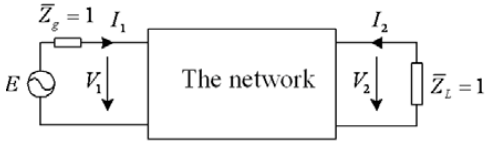

Figure 3. Network of antenna system.

Suppose both antenna 1 and antenna 2 are loaded with 50 Ω impedance, i.e., $\bar{Z}_g = \bar{Z}_l = \bar{Z}_0 = 1$, the isolation between antenna

1 and antenna 2 can be defined as

$$I = 10\log\left(\frac{P_i}{P_l}\right) = 10\log\frac{\mathrm{Re}\left(\bar{Z}_{11} - \dfrac{\bar{Z}_{12}^2}{\bar{Z}_{22}+1}\right)}{\left|\dfrac{\bar{Z}_{12}}{\bar{Z}_{22}+1}\right|^2} \tag{1}$$

Now we can see that the most important thing in the isolation

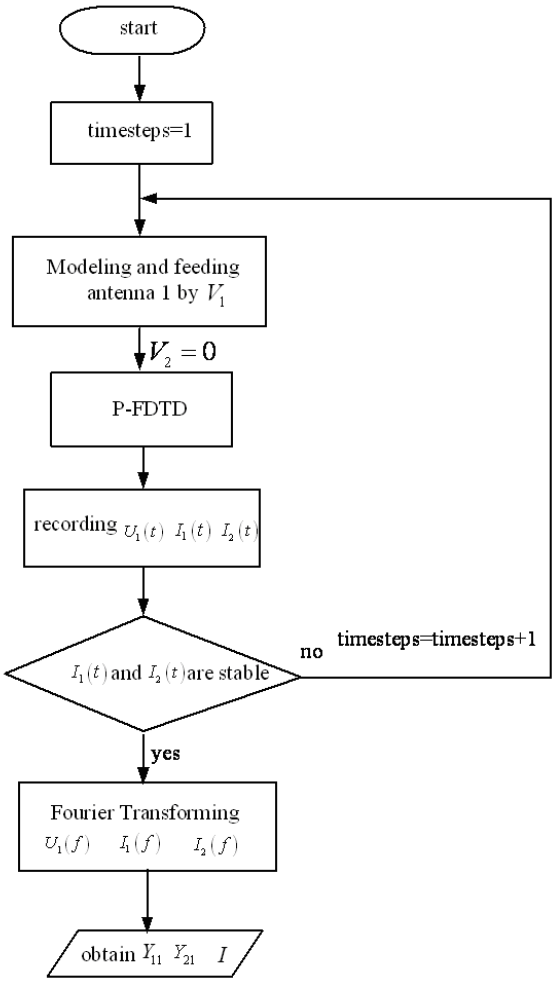

Figure 4. The flow process chart of the isolation.

analysis is to calculate the mutual impedance and self-impedance to obtain the S isolation of the Network.

2.3. Mechanism of Solving Isolation between Antennas Using Parallel FDTD

Take the two-port network for example. Antenna 1 and antenna 2 are fed by V_1 and V_2. In the case of $V_2 = 0$, The self-impedance and mutual impedance are defined as

$$\begin{cases} Y_{11} = \dfrac{I_1}{V_1}\Big|_{V_2=0} \\ Y_{21} = \dfrac{I_2}{V_1}\Big|_{V_2=0} \end{cases} \tag{2}$$

Then the mutual impedance and self-impedance can be obtained. Also the isolation between antennas can be computed. The flow process chart of the mechanism is shown in Fig. 4.

3. EXAMPLES FOR VALIDATION

3.1. The Radiation Pattern of a Monopole Mounted on a Cylinder and Square Combination

Consider a $\lambda/4$ monopole mounted on a cylinder (2.425λ-radius) and square (12.125λ-side) combination (Fig. 5). The increment $dx = dy = dz = \lambda/20$ is used here and the amount of the FDTD grids is

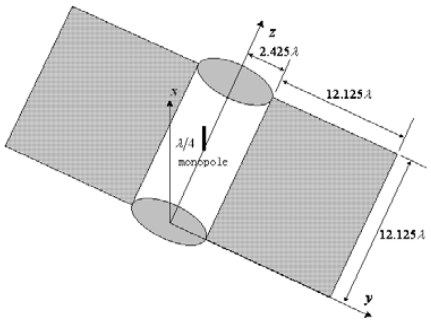

Figure 5. A cylinder and square combination.

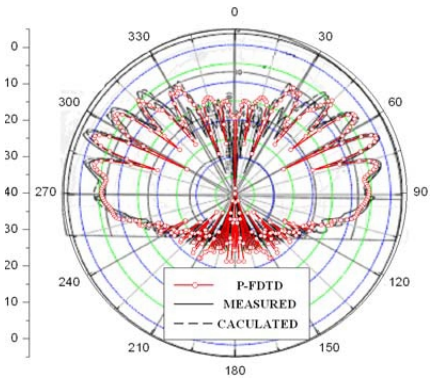

Figure 6. The radiation pattern of xoy plane.

$140 \times 620 \times 280$. Fig. 6 presents the radiation pattern of xoy plane using parallel FDTD, which agrees well with the measured and calculated results in the literature [19].

3.2. The Isolation of Two Monopoles Mounted on a Cylinder

In this case, the Parallel FDTD method is employed to simulate two $\lambda/4$ monopoles mounted on a cylinder with 0.5 m radius and 4.0 m height (see Fig. 7). The isolation between the two antennas is computed from 150 MHz to 450 MHz. The increment $dx = dy = dz = 0.0125$ m is used here and the amount of the FDTD grids is $140 \times 140 \times 360$. The isolation curve of the antennas is shown in Fig. 8. The Parallel FDTD curve is in good agreement with the result of MOM.

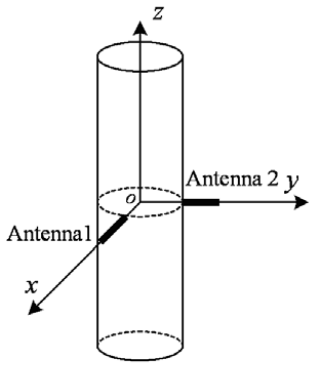

Figure 7. A cylinder.

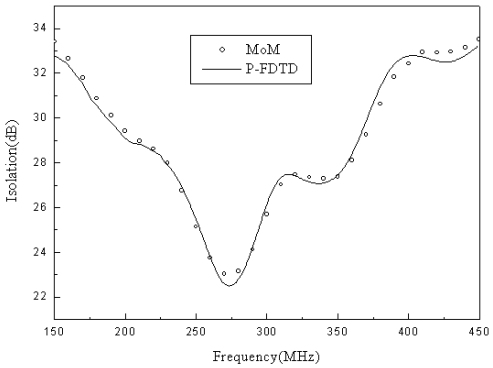

Figure 8. The isolation between antennas on a cylinder.

The current of antenna 2 converges when the time steps are 3000 and the computation time is about 1.05 hours. Contrastively, the computation of the isolation at 31 frequency points costs 22.32 hours using MOM. From the results above, it can be concluded that the Parallel FDTD can avoid the complexity of sweeping frequency and reduce the computing time greatly as a time-domain method.

4. EXAMPLES OF ELECTRICALLY LARGE PLATFORMS

4.1. Radiation Patterns and Isolation of Two Antennas Mounted on a Warship

We consider a $153 \times 15 \times 16.5$ m perfectly conducting warship whose FDTD models are shown in Fig. 9. Two $\lambda/4$ monopoles are mounted on the warship and the position is shown in Fig. 9. The radiation patterns are calculated at 30 MHz. The isolation is computed from 20 MHz to 60 MHz. So the increment $dx = dy = dz = 0.25$ m is used here and the amount of the FDTD grids is $660 \times 130 \times 180$. 8 nodes are used to build PC cluster. The total computational memory is about 2 GB and the memory per node is about 0.27 GB.

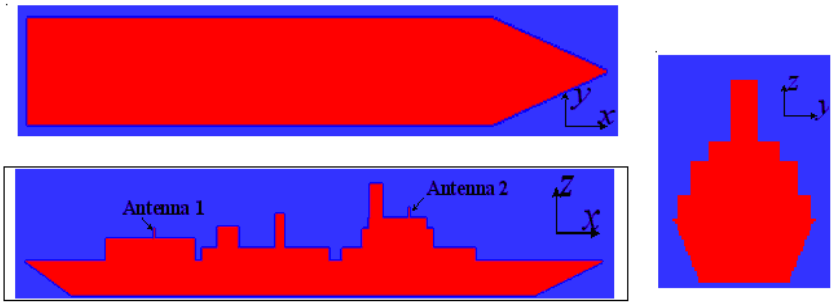

Figure 9. The three view charts of a warship with two antennas.

The radiation patterns are shown in Fig. 10. In the pattern of xoy plane, the fields in the fore and poop are less than those in the two sides of the warship because of the influence of the parts of the warship. It is symmetric because the antennas are mounted in the middle axle of the warship. In the pattern of xoz plane, the fields in the upper side is much more than in those lower side because the reflection of the warship body. For the pattern of yoz plane, the fields in upper side is more than those in lower side because of the same reason as xoz plane. It is symmetric too.

The isolation curve is shown in Fig. 11. The isolation between them is more than 30 dB from 20 MHz to 60 MHz. So it is can be concluded that the two antennas are in good isolated status.

The current converges when the time steps are 3000 and the computation time is about 2.18 hours.

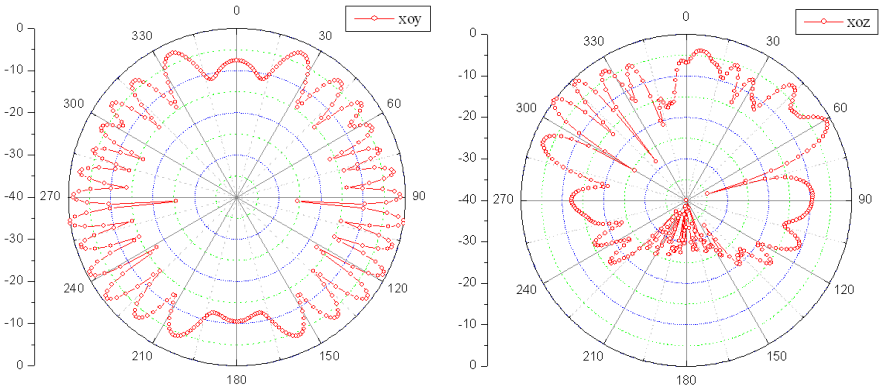

(a) The radiation pattern of *xoy* plane (b) The radiation pattern of *xoz* plane

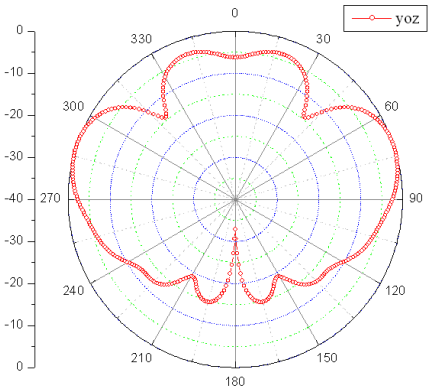

(c) The radiation pattern of *yoz* plane

Figure 10. The patterns of two antennas on a warship.

4.2. Radiation Patterns and Isolation of Three Antennas Mounted on a Warship

Three $\lambda/4$ monopoles are mounted on the warship and the position is shown in Fig. 12. The radiation patterns are calculated at 30 MHz. The isolation is computed from 20 MHz to 60 MHz. The increment and the amount of the FDTD grids are the same as above. 8 nodes are used to build PC cluster.

The radiation patterns of three antennas (see Fig. 13) are similar with the patterns of two antennas in Fig. 10. The isolation curves are shown in Fig. 14. The isolation between antenna 1 and antenna 3 is more than 30 dB. Then they have little coupling in the frequency

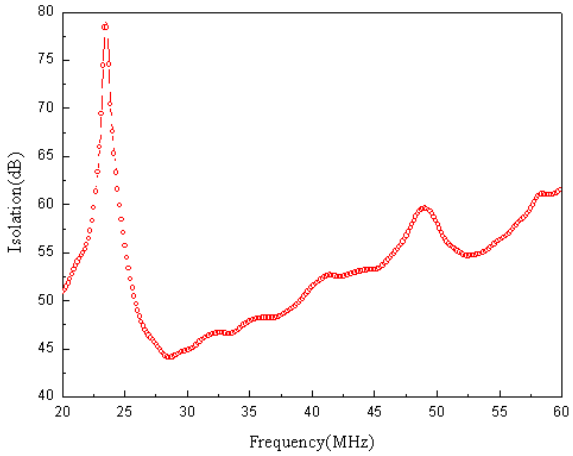

Figure 11. The isolation of two antennas on the warship.

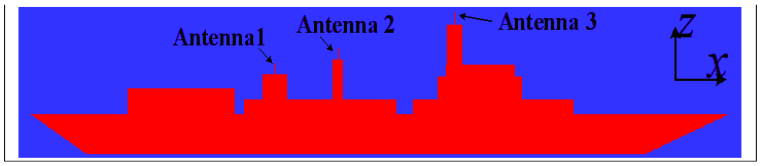

Figure 12. The side elevation of a warship with three antennas.

band. The isolation between antenna 2 and antenna 3 is less than 30 dB near 30 MHz so that the antennas has great coupling each other in the frequency band. Besides it is noticed that the isolation between antenna 2 and 3 is more than that between antenna 1 and 3 from 42 MHz to 45 MHz. It can be concluded that only increasing the distance between antennas can't reduce the coupling sometimes and other means should be carried out in the design. The coupling between antenna 1 and antenna 2 is great from 20 MHz to 45 MHz and becomes weak above 45 MHz.

4.3. Radiation Patterns and Isolation of a Monopole Mounted on Three Positions of a Plane

We consider a $46.59 \times 50.5 \times 14.76$ m perfectly conducting plane. One $\lambda/4$ monopole are mounted on the front, middle and back of a plane and the FDTD models are shown in Fig. 15. The radiation patterns are calculated at 50 MHz. The increment $dx = dy = dz = 0.15$ m is used here and the amount of the FDTD grids is $400 \times 120 \times 380$. Also 8

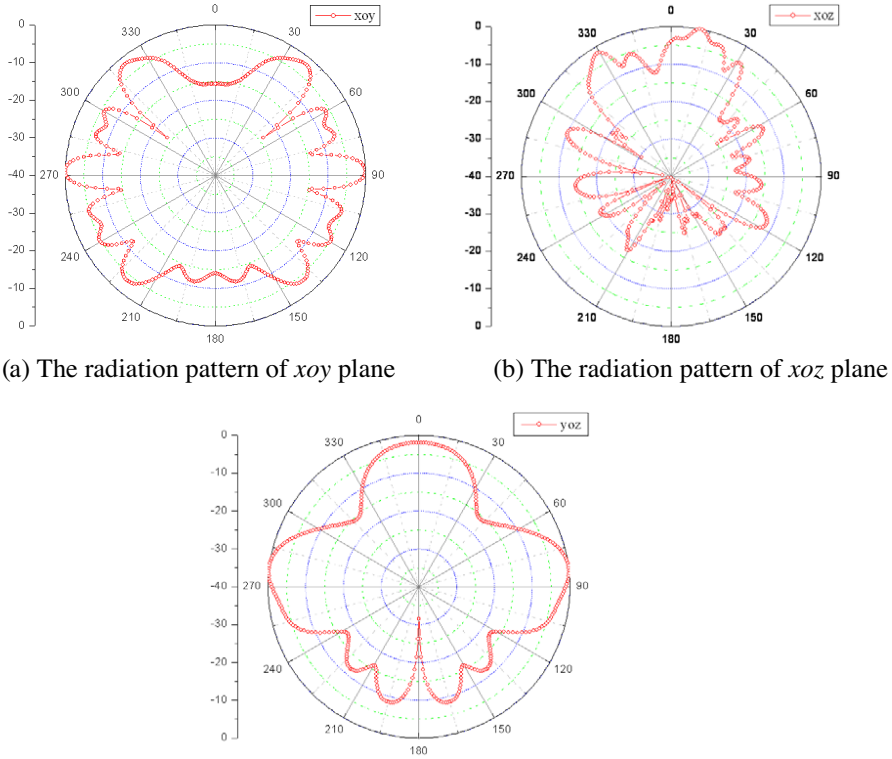

(a) The radiation pattern of *xoy* plane (b) The radiation pattern of *xoz* plane

(c) The radiation pattern of *yoz* plane

Figure 13. The patterns of three antennas on a warship.

nodes are used to build PC cluster. The total computational memory is about 3 GB and the memory per node is about 0.4 GB.

From the radiation patterns, we can see the influence of the plane on the antenna. The patterns of monopole mounted on the plane change greatly with the position.

4.4. Radiation Patterns and Isolation of Three Monopoles Mounted on a Plane

Three $\lambda/4$ monopoles are mounted on the plane and the position is shown in Fig. 17. The radiation patterns are calculated at 50 MHz. The isolation is computed from 20 MHz to 80 MHz. The increment and the amount of the FDTD grids are the same as above.

The radiation patterns are shown in Fig. 18 and the isolation curve is shown in Fig. 19. From the isolation curves, the isolation

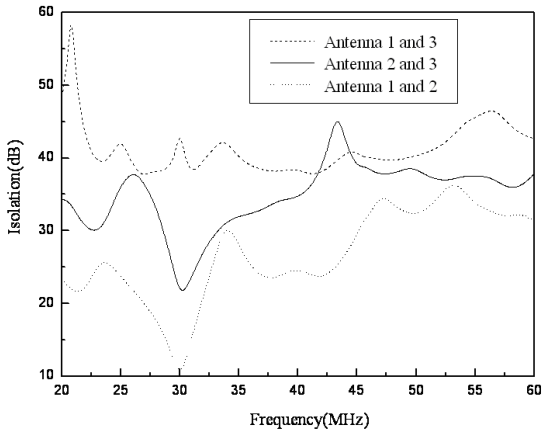

Figure 14. The isolation of three antennas on the warship.

between antennas changes greatly with the frequency and the positions of the antennas. In total, the isolation rises with the growth of the frequency. It is reasoned that the electrical distance becomes far as the frequency rises. The mutual coupling between antenna 1 and antenna 2 is intense since the isolation between them is less than 30 dB. The isolation between antenna 1 and antenna 3 is more than 30 dB because they are located in invisible areas and far away from each other. The isolation between antenna 2 and antenna 3 is good in all the frequency band except near 50 MHz. In the computation of isolation, the current converges when the time steps are 5000 and the computation time is about 3.42 hours.

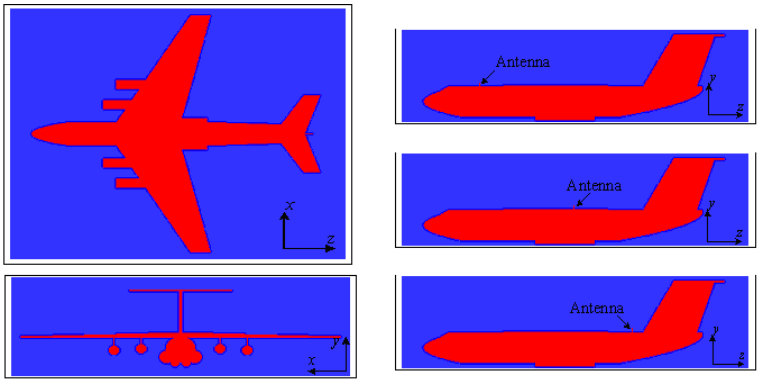

Figure 15. The three view charts of a plane with an antenna.

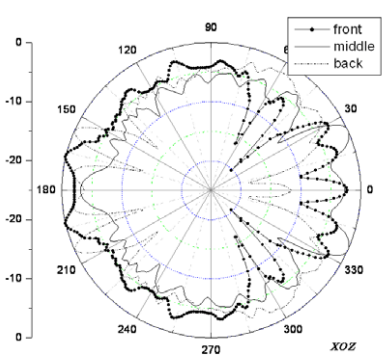

(a) The radiation pattern of *xoz* plane

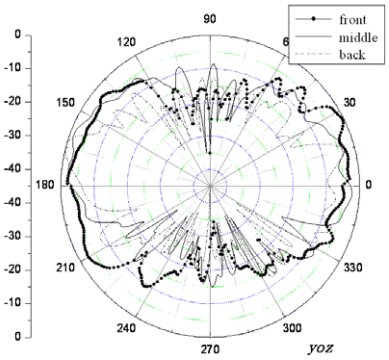

(b) The radiation pattern of *yoz* plane

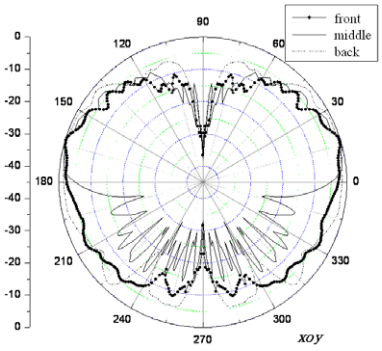

(c) The radiation pattern of *xoy* plane

Figure 16. The radiation patterns of an antenna on different position of the plane.

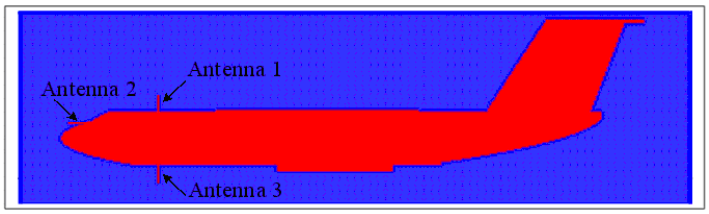

Figure 17. The side elevation of a plane with three antenna.

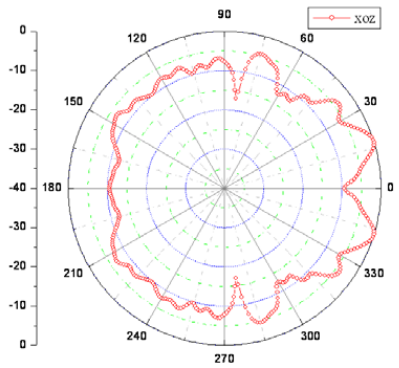

(a) The radiation pattern of *xoz* plane

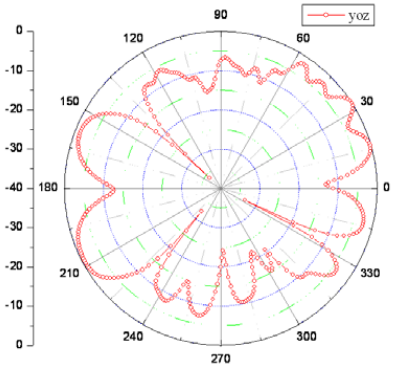

(b) The radiation pattern of *yoz* plane

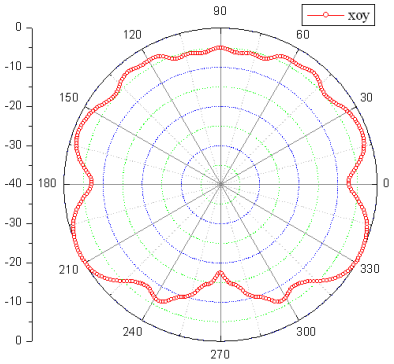

(c) The radiation pattern of *xoy* plane

Figure 18. The patterns of three antennas on the plane.

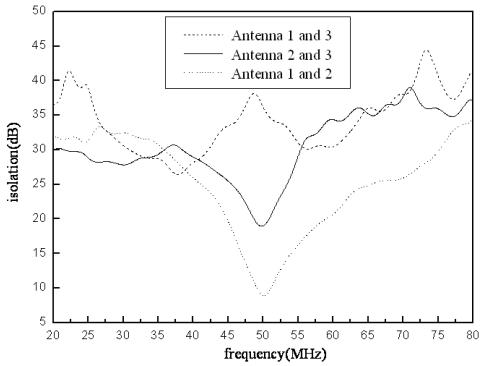

Figure 19. The isolation of three antennas on the plane.

5. CONCLUSTION

In this paper, the Parallel FDTD method based on MPI, a full-wave numerical method, is applied to analyze the EMC problems of the electrically large platforms. Parallel FDTD method can model the electrically large platforms accurately to analyze the EMC problems. The network theory is introduced to compute the isolation between antennas combined with the Parallel FDTD method firstly, which avoids the complexity of sweeping frequency and reduce the computing time greatly. Follow two examples for validation, the EMC problems of electrically large platforms are analyzed and some useful conclusions are obtained.

REFERENCES

1. Rao, S. M., D. R. Wilton, and A. W. Glisson, "Electromagnetic scattering by surfaces of arbitrary shape," *IEEE Trans. Antennas Propagat.*, Vol. 30, No. 5, 409–418, 1982.
2. Dos Santos, M. L. X. and R. R. Nilson, "On the Ludwig integration algorithm for triangular subreqions," *Proceedings of the IEEE*, Vol. 74, No. 10, 1455–1456, 1986.
3. Kouyoumijian, R. G. and P. G. A. Pathak, "Uniform geometrical diffraction for an edge in a perfectly conducting surfaces," *Proceedings of the IEEE*, Vol. 62, No. 11, 1448–1461, 1974.
4. Zhao, X. W., X. J. Dang, Y. Zhang, and C. H. Liang, "MLFMA analysis of waveguide arrays with narrow-wall slots," *Journal of Electromagnetic Waves and Applications*, Vol. 21, No. 8, 1063–1077, 2007.
5. Yee, K. S., "Numerical solution of initial boundary value problems involving Maxwell's equations in isotropic media," *IEEE Trans. Antennas Propagat.*, Vol. 14, 302–307, 1966.
6. Hu, X.-J. and D.-B. Ge, "Study on conformal FDTD for electromagnetic scattering by targets with thin coating," *Progress In Electromagnetics Research*, PIER 79, 305–319, 2008.
7. Qian, Z. H., R.-S. Chen, K. W. Leung, and H. W. Yang, "FDTD analysis of microstrip patch antenna covered by plasma sheath," *Progress In Electromagnetics Research.*, PIER 52, 173–183, 2005.
8. Liu, Y., Z. Liang, and Z. Yang, "Computation of electromagnetic dosimetry for human body using parallel FDTD algorithm combined with interpolation technique," *Progress In Electromagnetics Research*, PIER 82, 95–107, 2008.
9. Wang, M. Y., J. Xu, J. Wu, Y. Yan, and H.-L. Li, "FDTD

study on scattering of metallic column covered by double-negative metamaterial," *Journal of Electromagnetic Waves and Applications*, Vol. 21, No. 14, 1905–1914, 2007.

10. Lu, W. and T. Cui, "Efficient method for full-wave analysis of large-scale finite-sized periodic structures," *Journal of Electromagnetic Waves and Applications*, Vol. 21, No. 14, 2157–2168, 2007.
11. Zhang, Y., J. Song, and C. Liang, "MPI based parallelized locally conformal FDTD for modelling slot antennas and new periodic structures in microstrip," *Journal of Electromagnetic Waves and Applications*, Vol. 18, No. 10, 1321–1335, 2004.
12. Zhang, Y., J. Song, and C. Liang, "Study on the parallel modified locally conformal FDTD algorithm on cluster of PCs for PBG structures," *Acta Electronica Sinica*, Vol. 31, No. 12A, 2142–2144, 2003.
13. Lei, J. Z., C. H. Liang, and Y. Zhang, "Study on shielding effectiveness of metallic cavities with apertures by combining parallel FDTD method with windowing technique," *Progress In Electromagnetics Research*, PIER 74, 85–112, 2007.
14. Park, J. K., D. H. Shin, J. N. Lee, and H. J. Eom, "A full-wave analysis of a coaxial waveguide slot bridge using the Fourier transform technique," *Journal of Electromagnetic Waves and Applications*, Vol. 20, No. 2, 143–158, 2006.
15. Liu, Y., Z. Liang, and Z. Yang, "A novel FDTD approach featuring two-level parallelization on PC cluster," *Progress In Electromagnetics Research.*, PIER 80, 393–408, 2008.
16. Guiaut, C. and K. Mahdjoubi, "A parallel FDTD algorithm using the MPI library," *IEEE Antennas and Propagation Magazine*, Vol. 43, No. 2, 94–103, April 2001.
17. Li, L.-W., Y.-J. Wang, and E.-P. Li, "MPI-based parallelized precorrected FFT algorithm for analyzing scattering by arbitrarily shaped three-dimensional objects," *Progress In Electromagnetics Research*, PIER 42, 247–259, 2003.
18. Andersson, U., "Time-domain methods for the Maxwell equations," Doctoral Dissertation, Royal Institute of Technology, Sweden, 2001.
19. NASA REPORT No. 710816-8.